



# ATLAS LAr Calorimeter Performance in LHC Run 2

---

Devin Mahon, on behalf of the ATLAS Liquid Argon Calorimeter Group  
February 26, 2020  
INSTR20



# Outline



---

- Detector Overview
- Data Quality
- Run 2 Studies:
  - ▶ Purity Stability
  - ▶ Pulse Shapes
  - ▶ Energy Resolution
  - ▶ Timing
- Phase I Upgrade for Run 3

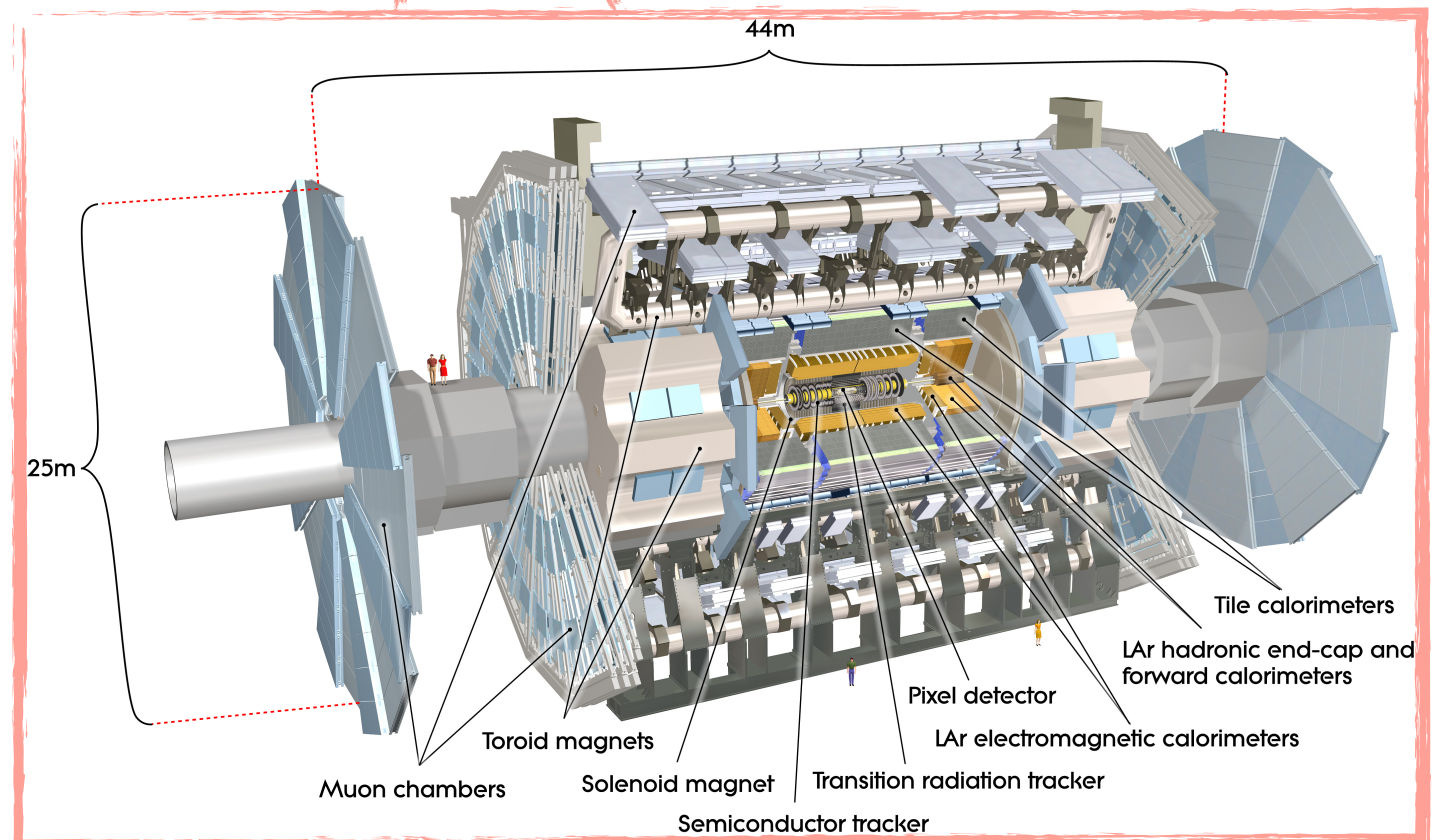
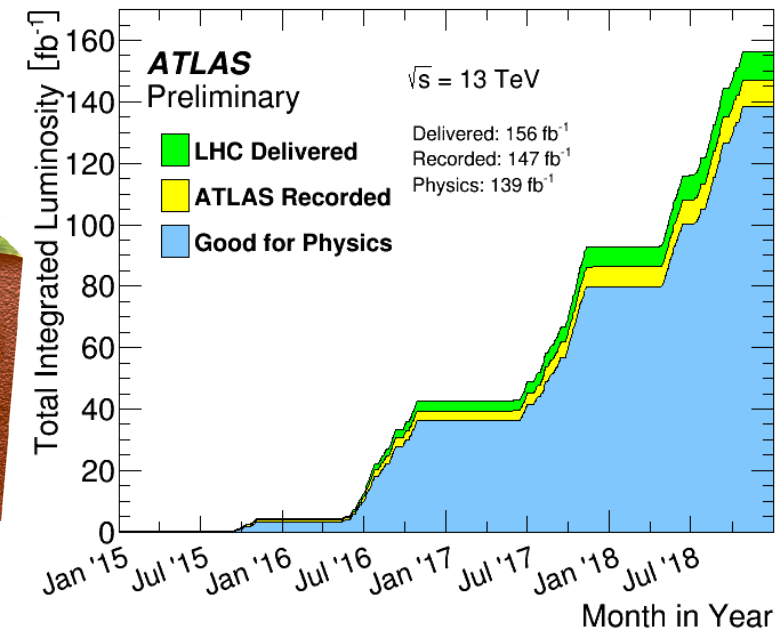
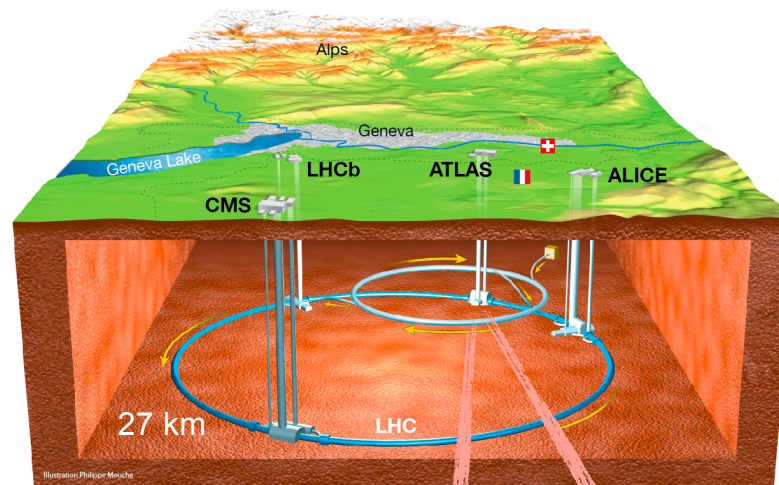
# ATLAS and the LHC

- CERN's Large Hadron Collider (LHC)

- ▶ Proton-proton (pp) and heavy ion collision modes
- ▶ Center-of-mass energy:  $\sqrt{s} = 13$  TeV
- ▶ Bunch crossing rate: 40 MHz
- ▶ Peak luminosity in Run 2 (2015-2018):  $2.1 \times 10^{34} \text{ cm}^{-2}\text{s}^{-1}$
- ▶ Pileup ( $\mu$ , interactions per bunch crossing):  $\bar{\mu} = 33.7$ ,  $\mu_{\text{max}} \sim 80$

- ATLAS

- ▶ One of two general-purpose detectors at the LHC
- ▶ Tracking, calorimetry, muon spectrometry
- ▶  $139 \text{ fb}^{-1}$  of recorded data good for physics in Run 2 ( $\sim 89\%$  efficiency)





# ATLAS Liquid Argon (LAr) Calorimeter

- Liquid argon sampling calorimeter

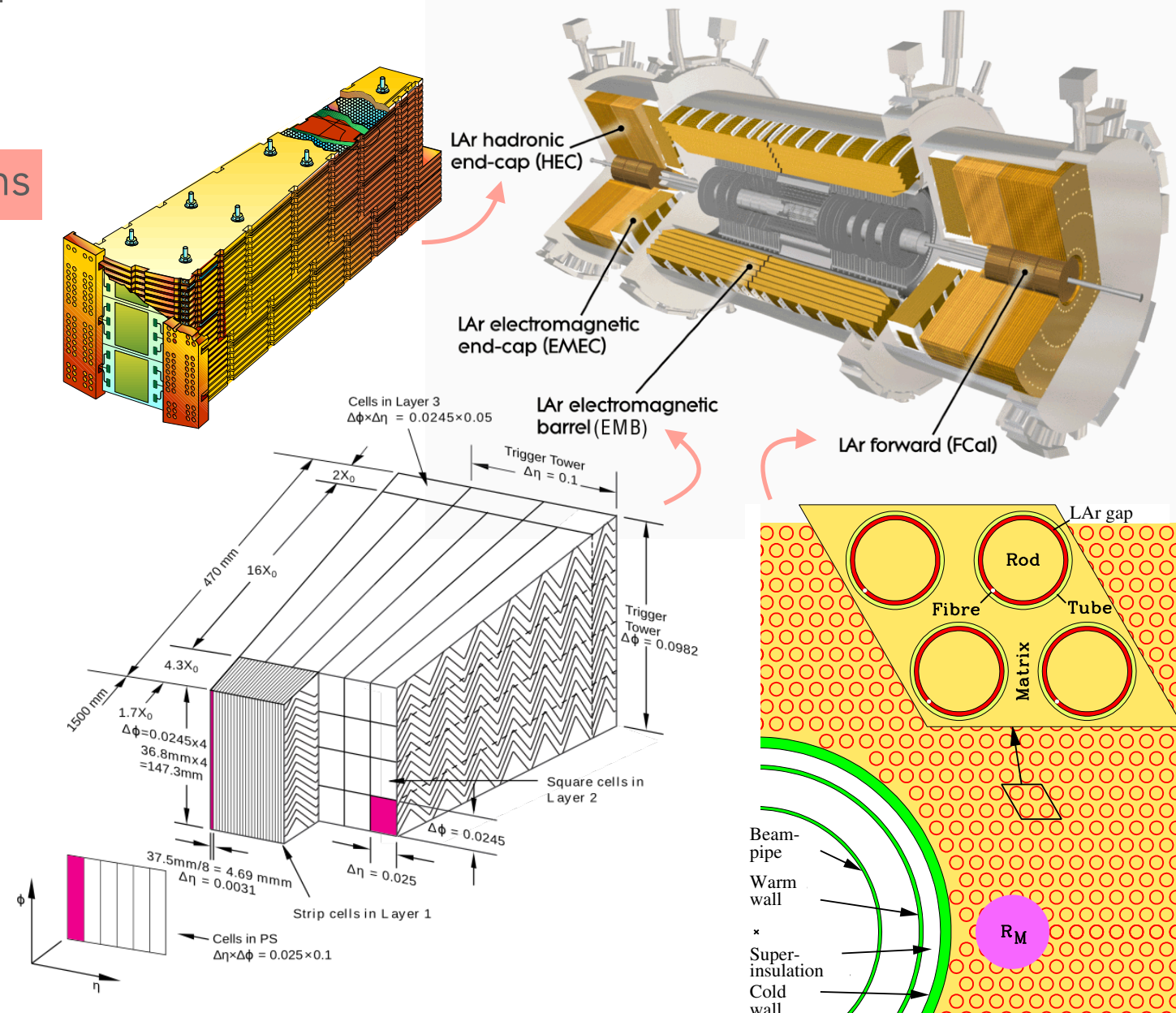
- ▶ Cooled with 3 cryostats to  $\sim 90$  K
- ▶ Linear response, uniform, stable, radiation-tolerant
- ▶  $\sim 182,000$  channels ( $>99.9\%$  operational)

- Electromagnetic (EM) and hadronic sections

- ▶ EM barrel (EMB) and end-cap (EMEC)
  - ▶ Lead plates interspaced as the passive material
  - ▶ Arranged in accordion-like structures
  - ▶ Fast readout and full, uniform azimuthal coverage
- ▶ Forward calorimeters (FCal)
  - ▶ Copper and tungsten absorber matrices with rod electrode structures
- ▶ Hadronic end-cap (HEC)
  - ▶ Conventional parallel copper plate electrodes

Detector component	Required resolution
EM calorimetry	$\sigma_E/E = 10\%/\sqrt{E} \oplus 0.7\%$
Hadronic calorimetry (jets)	
barrel and end-cap	$\sigma_E/E = 50\%/\sqrt{E} \oplus 3\%$
forward	$\sigma_E/E = 100\%/\sqrt{E} \oplus 10\%$

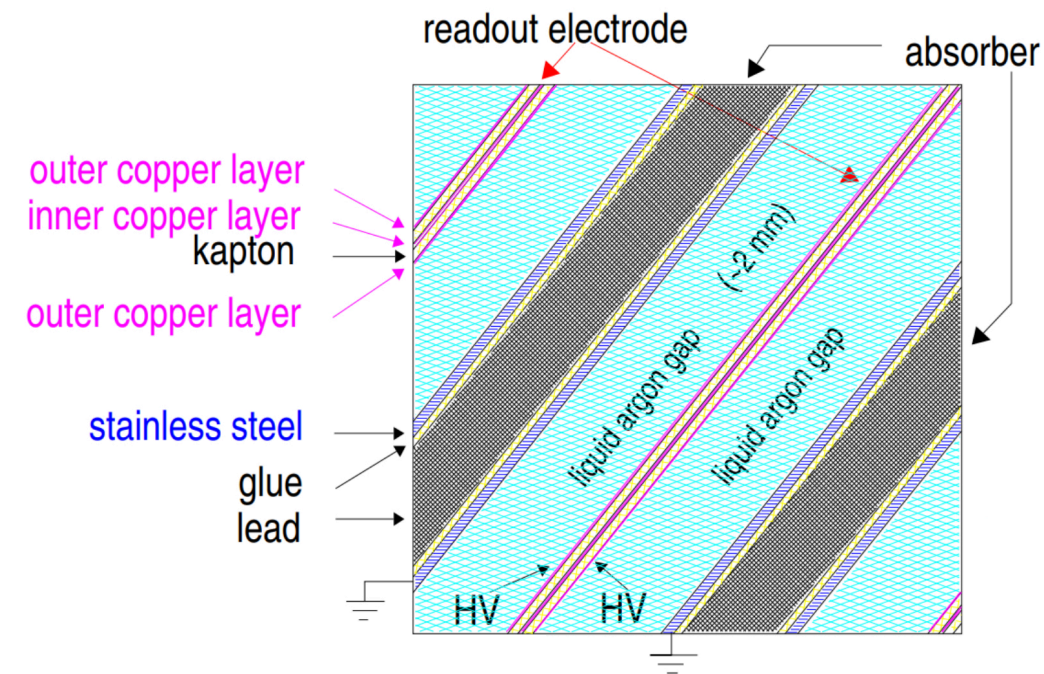
	Coverage in Pseudorapidity ( $\eta$ )
EMB	$ \eta  < 1.475$
EMEC	$1.375 <  \eta  < 3.2$
HEC	$1.5 <  \eta  < 3.2$
FCal	$3.1 <  \eta  < 4.9$



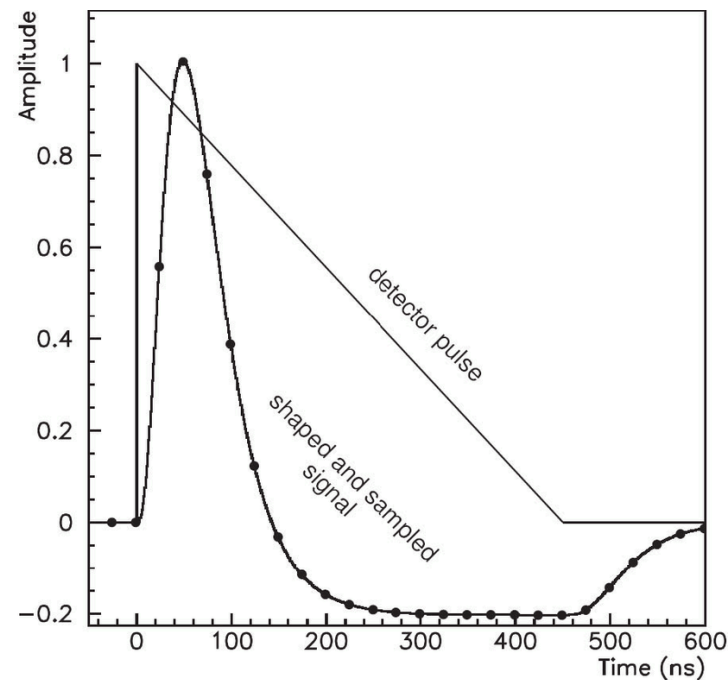


# Signal Measurement & Readout

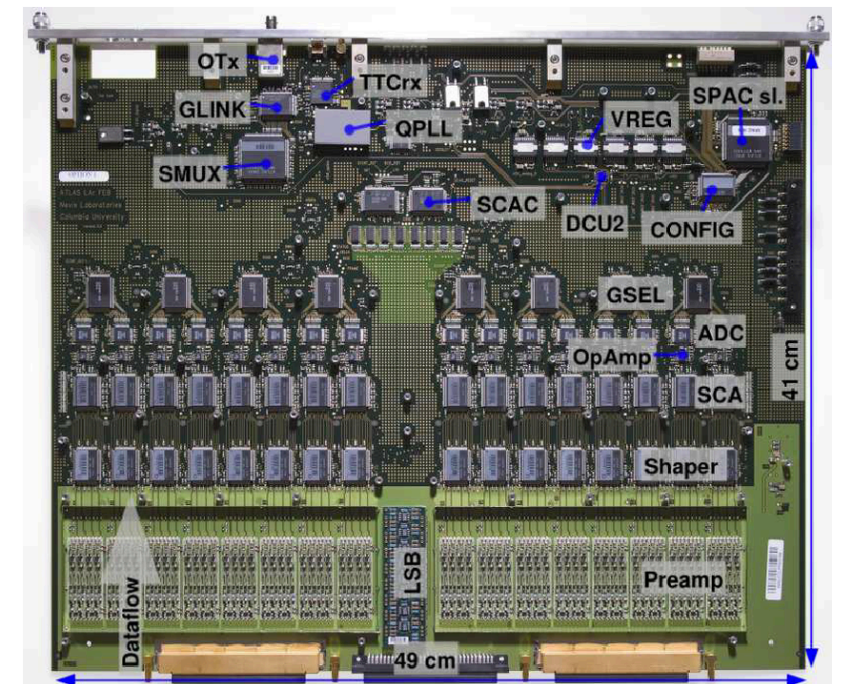
## Signal Production & Collection



## Ionization Pulse



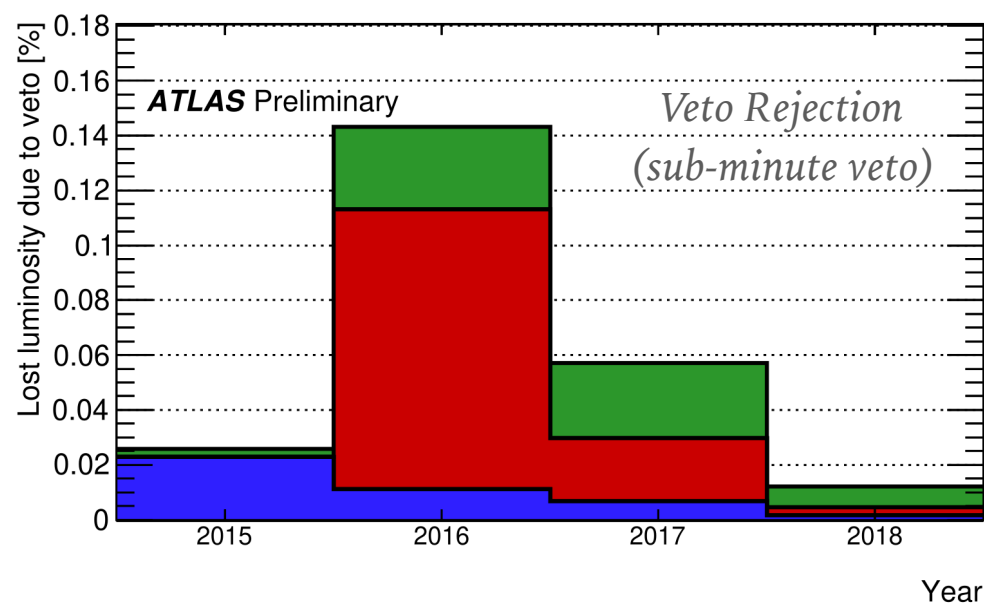
## Front-End Board



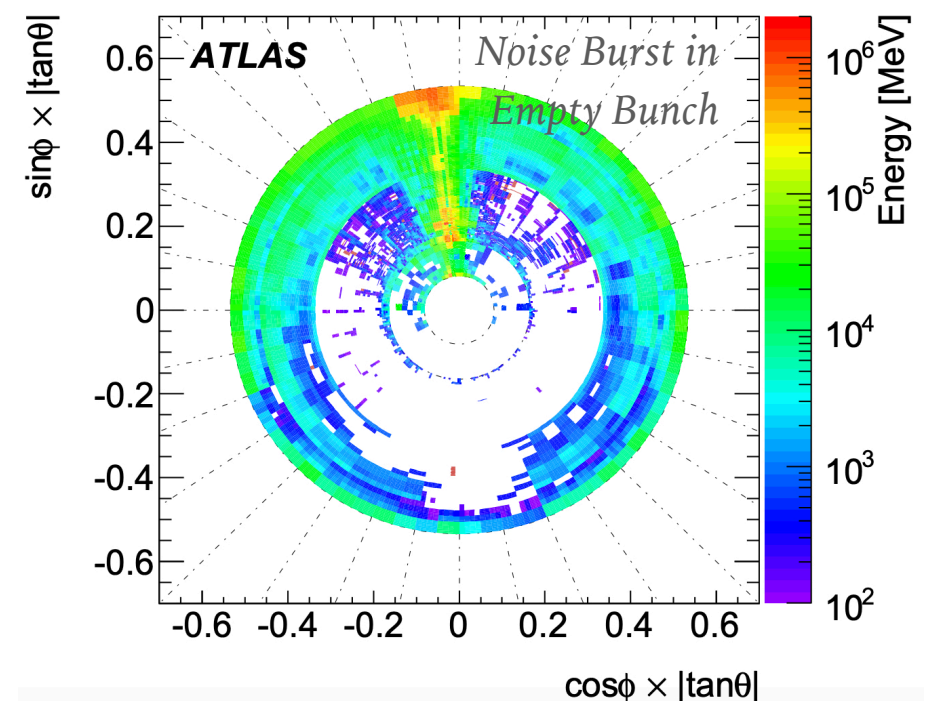
- **Signal production**
  - Incoming EM particle hits lead absorber, producing a shower in LAr, whose current is collected by electrodes
- **On-detector electronics**
  - Signal is amplified, split into 3 overlapping linear gain scales, and shaped on Front-End Boards (FEBs)
  - Sampled at 40 MHz and stored in analog buffer awaiting trigger decision
  - If triggered, gain is selected, and 4 samples are digitized and read out via optical fiber
- **Off-detector electronics**
  - Using optimal filtering coefficients (OFCs), amplitude (~energy) and time are computed
  - Quality factor measures consistency with in-time pulse, mitigates effects of out-of-time pileup

# LAr Offline Data Quality

- 99.6% overall data-taking efficiency for LAr in Run 2
- 2 categories of inefficiencies:
  - Defect rejection: reject full “long” block of data ( $> 1$  min.)
  - Veto rejection: issues in a “short” time period ( $< 1$  min.), reject event-by-event
- Main veto rejection data losses:
  - Noise bursts
    - Well-studied noise phenomenon affecting a large fraction of the detector for a short time ( $\sim 1$   $\mu$ s)
    - Suspected to be induced by unshielded HV cables
  - Mini noise bursts
    - Noise in a small region of the detector for a very short time (tens of ns)
    - Improved identification and HV tuning virtually eliminated their effect by 2018



	2015	2016	2017	2018
Luminos. :	3.4 fb <sup>-1</sup>	34.3 fb <sup>-1</sup>	45.5 fb <sup>-1</sup>	61.2 fb <sup>-1</sup>
Total loss:	0.03%	0.14%	0.06%	0.01%
data corruption	0.00%	0.03%	0.03%	0.01%
mini noise burst	-	0.10%	0.02%	0.00%
noise burst	0.02%	0.01%	0.01%	0.00%



# LAr Offline Data Quality

- Main defect rejection data losses:

- Noisy channels

- Individual channels masked due to noise from pulses incompatible with LAr ionization

- Noise bursts

- Previously discussed widespread coherent noise phenomenon

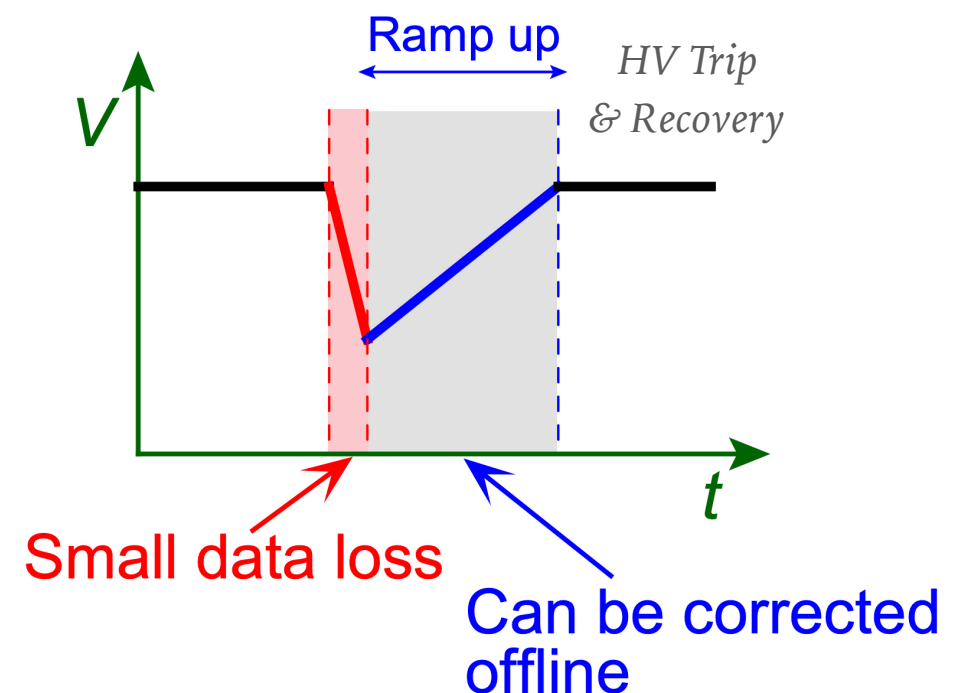
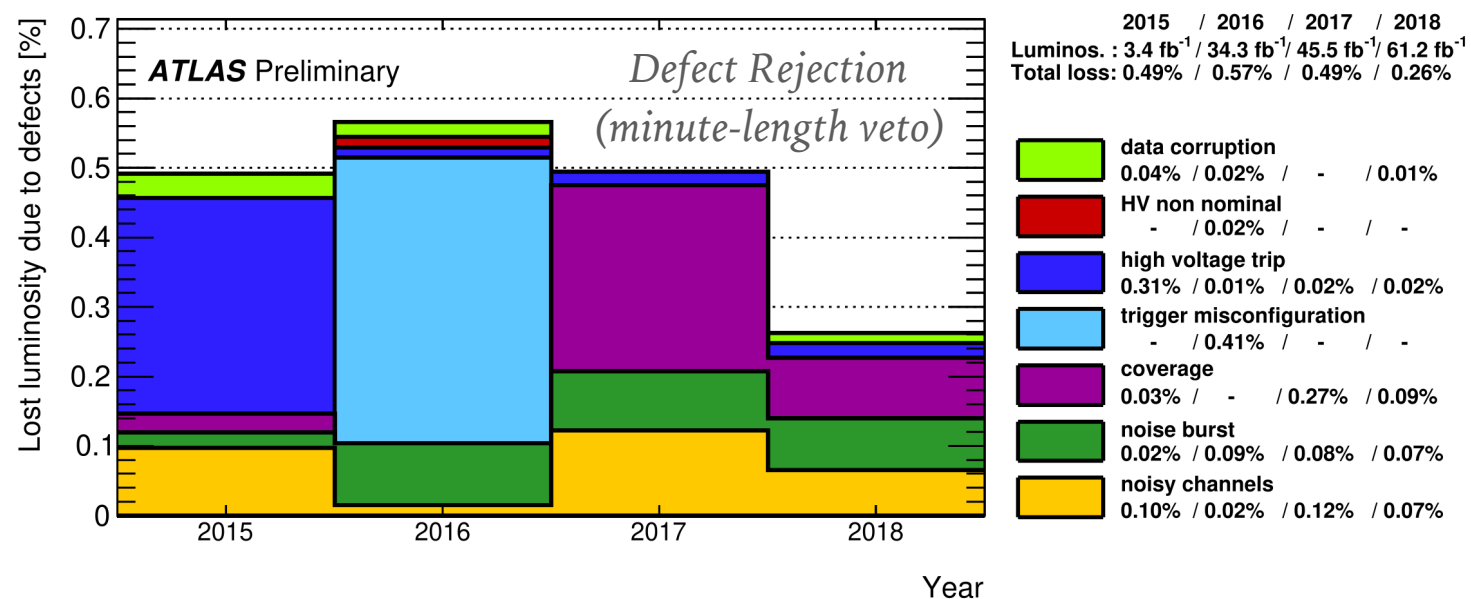
- Coverage

- Temporary improper readout in an area of >512 cells due to a single hardware failure

- High voltage (HV) trip

- Sudden HV drop making energy correction unreliable

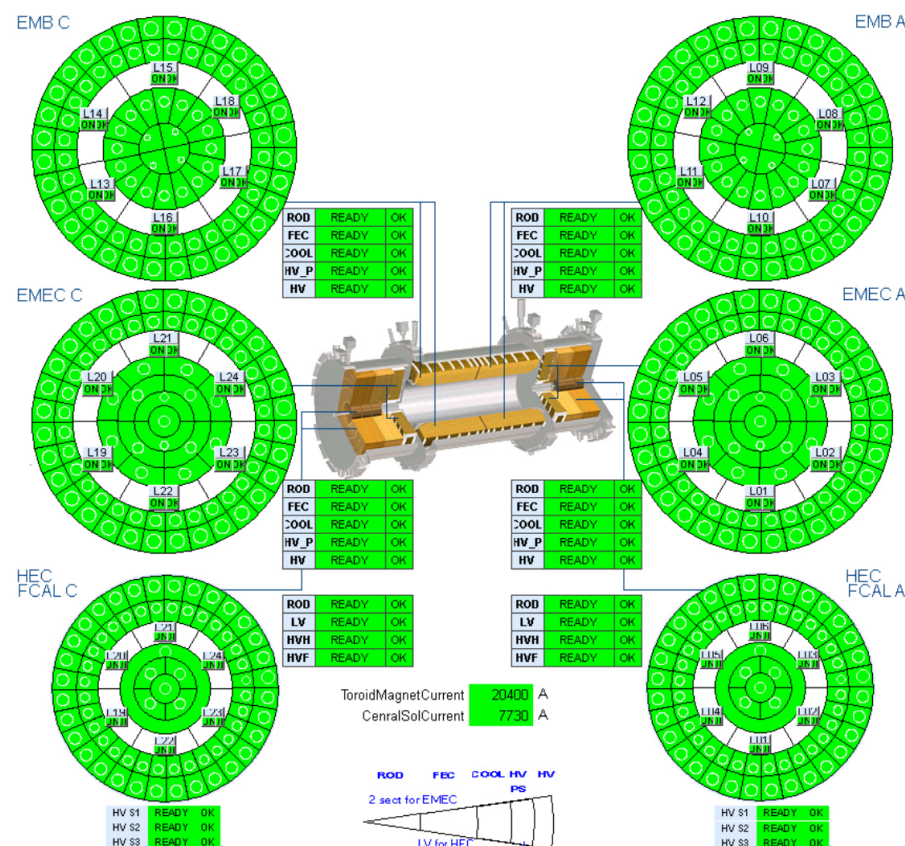
- Reduced significantly with new power supplies in 2016



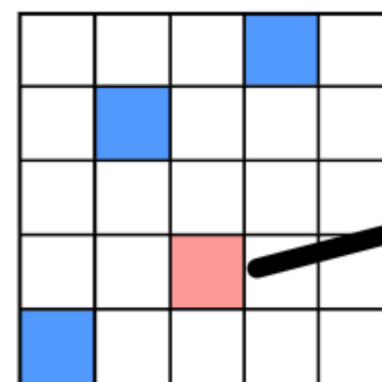


# Online Tools & Operations

- High efficiency and smooth operations thanks to:
  - Very stable system performance and a dedicated operations team
  - Real-time (online) monitoring tools to quickly identify issues
    - Noise, timing, trigger rates, and other data integrity checks
    - Configuration and hardware status
  - Automated recovery procedures
    - e.g. LAr Trigger Tower Noise Killer (LTTNK): automatically searches for and disables noisy cells from being used in Level-1 trigger

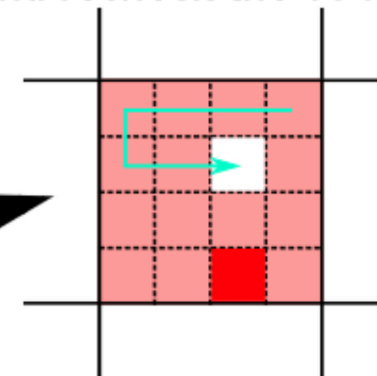


In case of trigger tower with too high rates

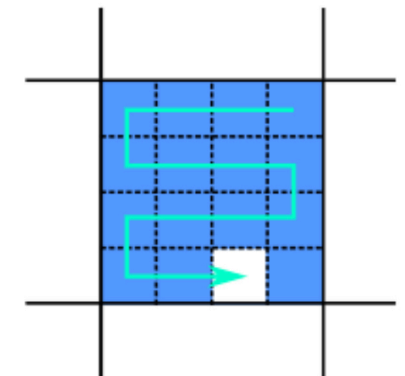


C. Camincher CALOR 2018

LTTNK disables cells of the tower one by one and recheck the TT rate



Until it finds the cell causing the noise



# Purity Stability Studies

- LAr impurities:

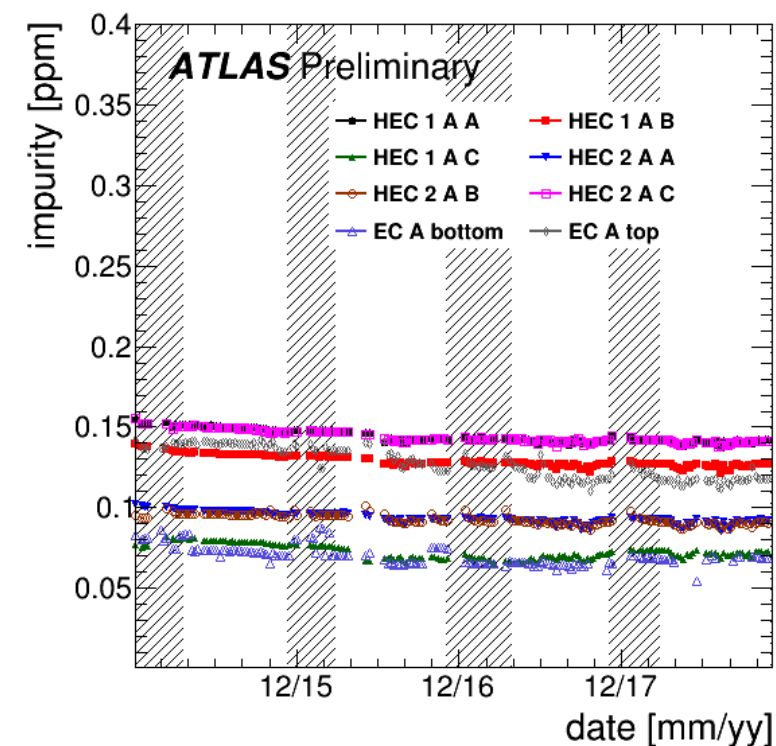
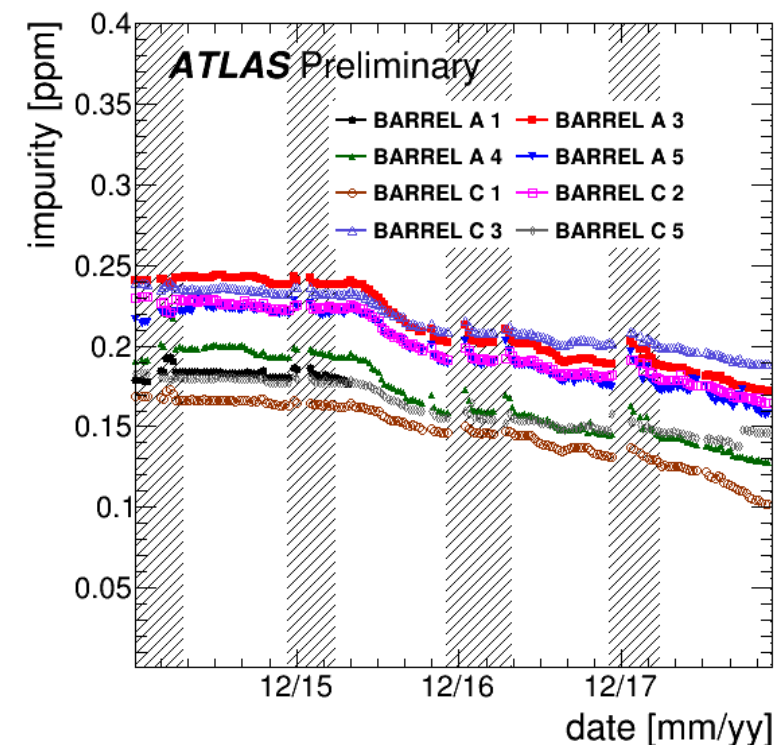
- ▶ Electronegative molecules (primarily O<sub>2</sub> and N<sub>2</sub>) capture signal electrons, preventing them from being collected at the electrodes
- ▶ Reduces signal-to-noise ratio
- ▶ Must be monitored to ensure good, stable conditions

- Impurity measurement:

- ▶  $\alpha$ - and  $\beta$ -source chambers in the cryostats measure electron lifetime in LAr
- ▶ Laser chambers in contact with LAr measure electron lifetime and drift velocity and provide calibration for source chambers
- ▶ Measured in oxygen equivalent
- ▶ Measurements during collisions excluded due to signals from radiation in the ionization chambers

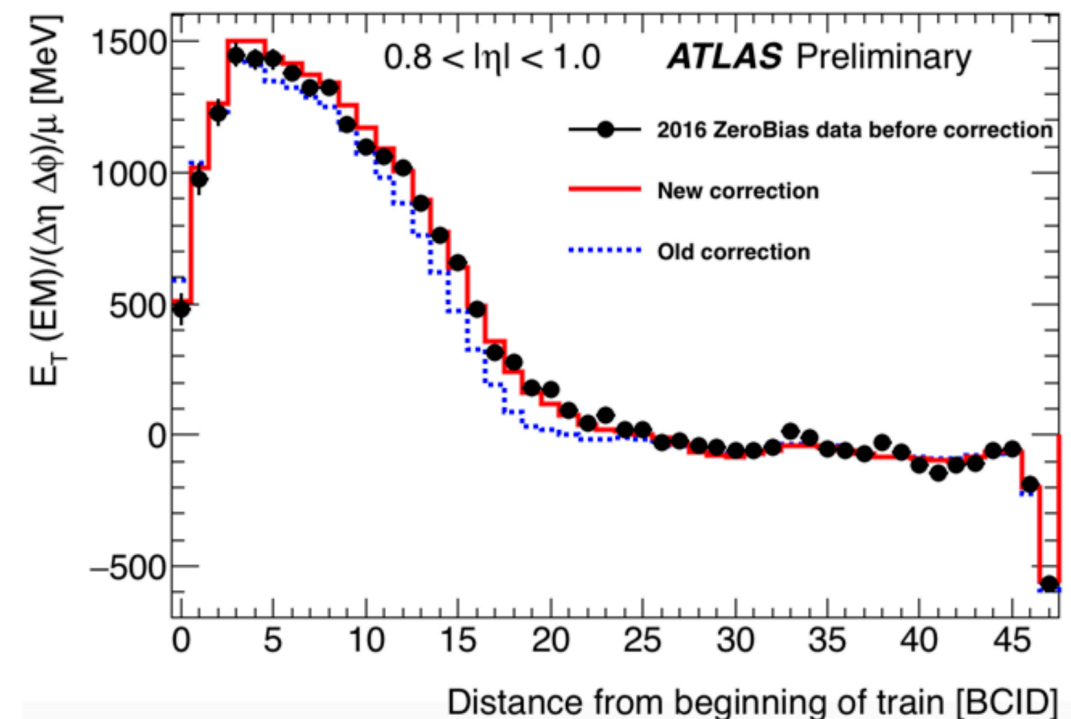
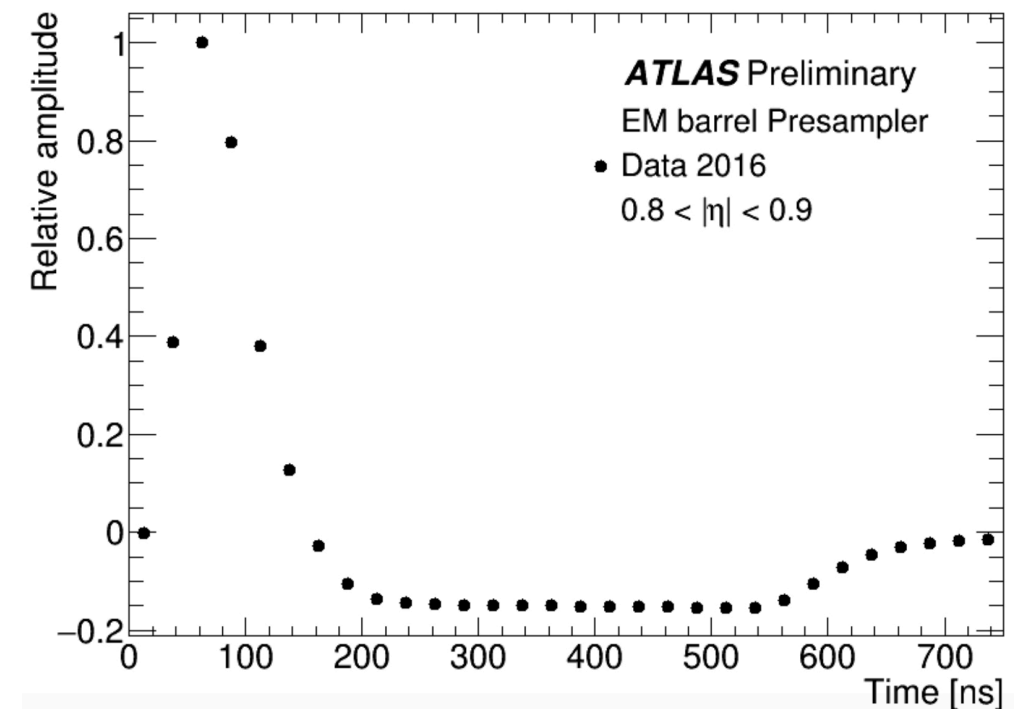
- Impurity remained stable in Run 2 for the end-caps and decreased for the barrel

- ▶ Always < 0.25 ppm
- ▶ Clear explanation for decrease unknown, but change of other input parameters (e.g. temperature or HV of the ionization chambers) is excluded



# Pulse Shape Studies

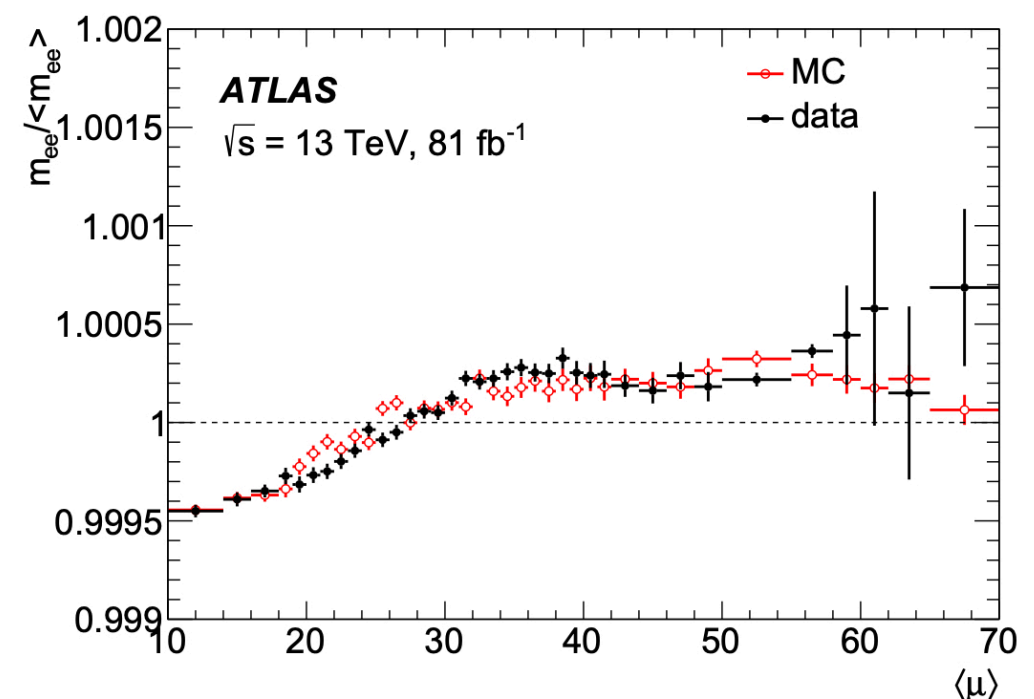
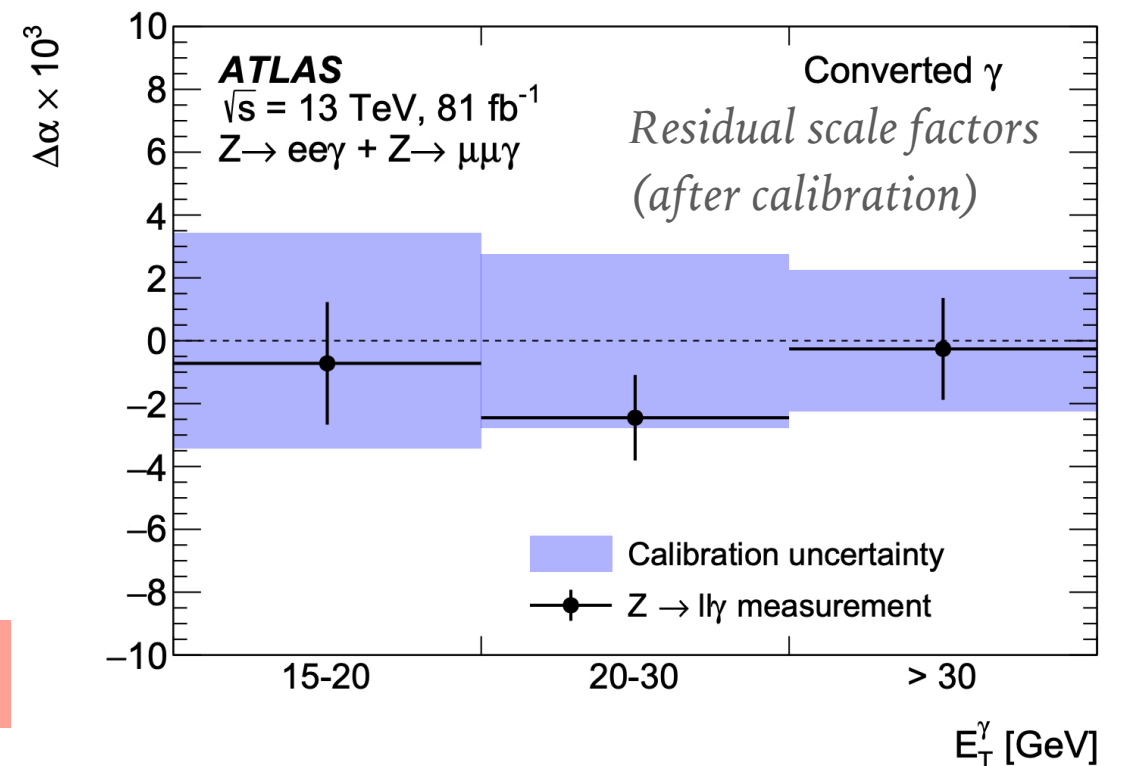
- Dedicated measurements taken during special runs
  - ▶ 2016: 4 samples recorded with random trigger around a single colliding bunch
  - ▶ 2017 & 2018: 32 samples recorded, shifting readout in steps of  $\sim 3$  ns
  - ▶ Physics pulse shape now sampled precisely at 256 points in various detector regions
- Precise knowledge of the pulse shape is important to:
  - ▶ Reduce uncertainties on shape corrections in energy computation
  - ▶ Cross-check LAr purity by examining distortions in the tail of the pulse caused by captured electrons
  - ▶ Improve the baseline correction for bunch structure
    - ▶ Bipolar pulse shape cancels in- and out-of-time pileup contributions to energy for infinite bunch trains
    - ▶ But finite trains and different bunch structures cause an energy shift
    - ▶ Applied as a pedestal correction
    - ▶ For a typical EM cluster and pileup, maximum baseline shift  $\sim 800$  MeV, reduced to  $< 30$  MeV after correction





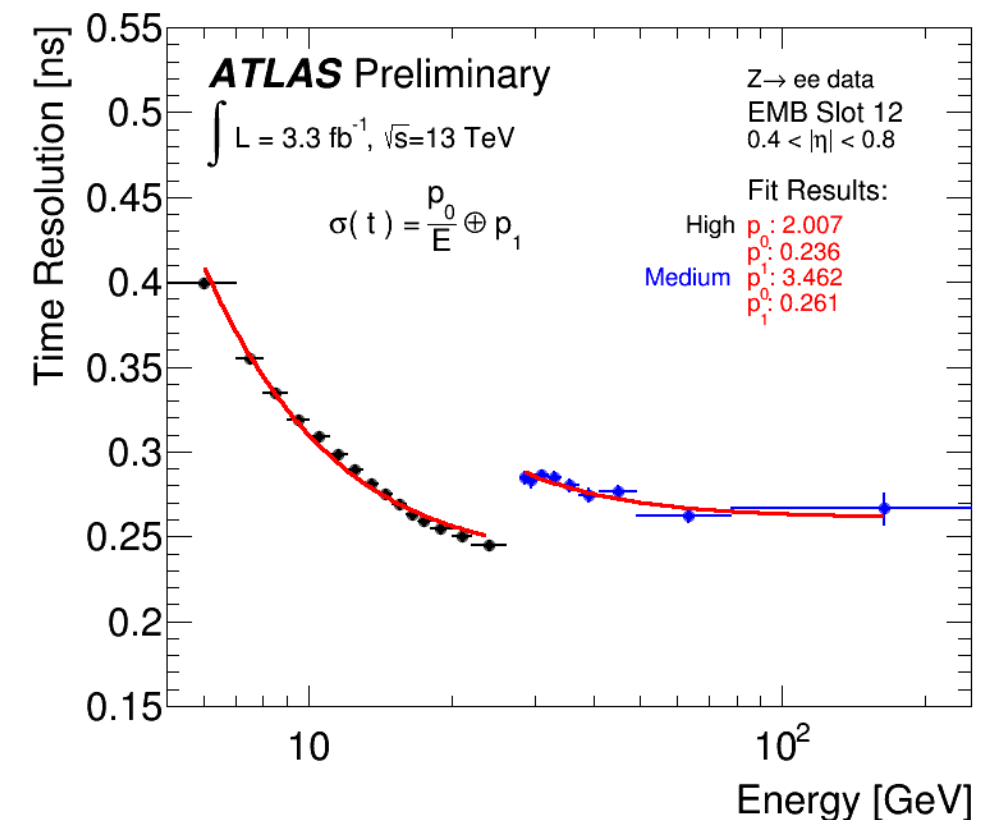
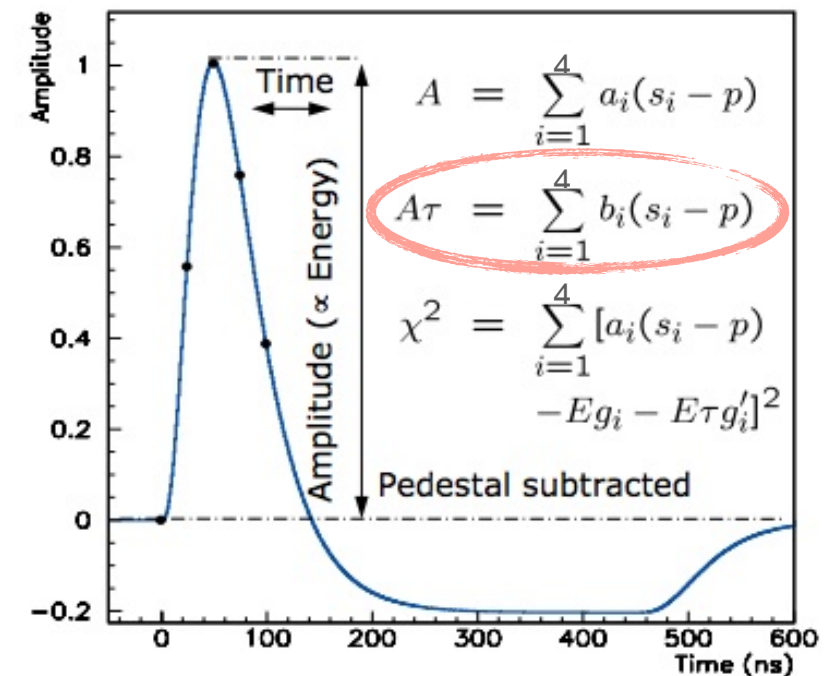
# Energy Resolution Studies

- Modeling of energy resolution
  - ▶ Mis-modeling of energy scale and resolution calibrated with  $Z \rightarrow ee$  data and MC
  - ▶ Corrections verified with  $Z \rightarrow ee\gamma$  and  $Z \rightarrow \mu\mu\gamma$  data with precision  $\lesssim 0.5\%$
- Higher pileup ( $\mu$ ) increases noise and thus worsens the energy resolution ( $\propto \sqrt{\mu}$ )
  - ▶ Stability is especially relevant for Run 3 and beyond with much higher pileup environments
  - ▶ Overall stability with  $Z \rightarrow ee$  data: within  $\sim 0.05\%$



# Timing Studies

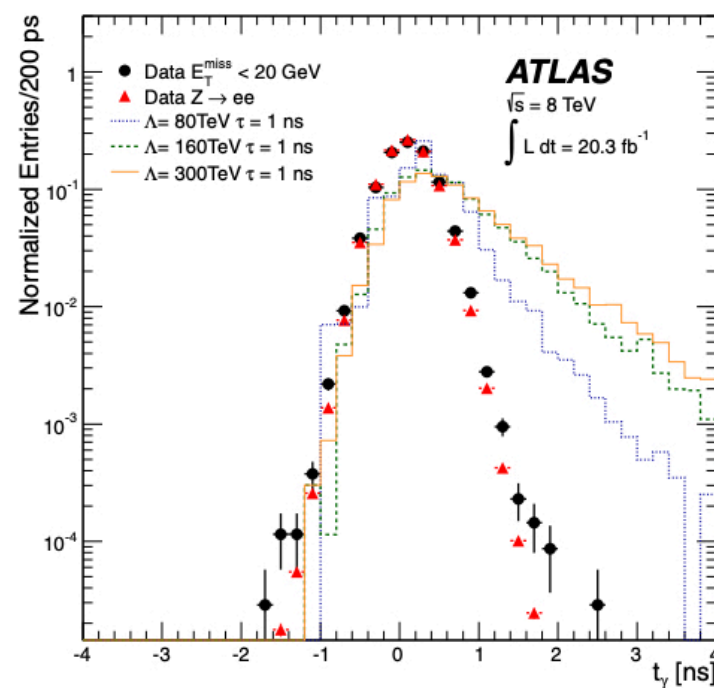
- Timing is calculated online with  $\sim 1$  ns resolution
  - Computed using optimal filtering coefficients (OFCs)
  - Tuned with FEB fine delays and monitored during data-taking
  - Sufficient for triggering and vetoing background
- Performance is significantly improved offline via calibration with electrons from W and Z boson decays
  - Removes timing variations from known detector effects
  - Improves resolution to as low as  $\sim 220$ - $270$  ps for high-energy electrons and photons
  - Powerful discriminant for long-lived particle searches
  - Computed beam spread timing component:  $\sim 200$  ps
- Uncorrelated contribution to constant term ( $p_1$ ) attributed to LAr:  $\sim 65$ - $185$  ps (varies in  $\eta$  and gain)
- LAr provides the most precise timing in ATLAS
  - New, updated calibration improves performance even further (results not yet released)



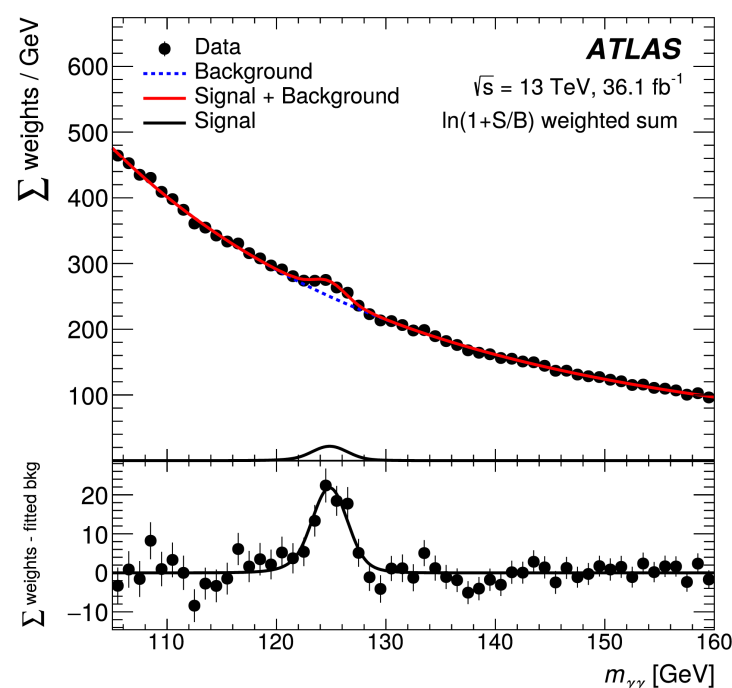
# LAr Calorimeter Physics Applications

- Provides precise measurements of EM objects for a wide variety of crucial applications
  - Higgs discovery and precision measurements:
    - $H \rightarrow \gamma\gamma, H \rightarrow ZZ^* \rightarrow 4e, H \rightarrow WW^* \rightarrow e\bar{\nu}e\nu$
    - Many searches for physics beyond the Standard Model
- Provides strong rejection of jet background and measurement of the EM component of jets

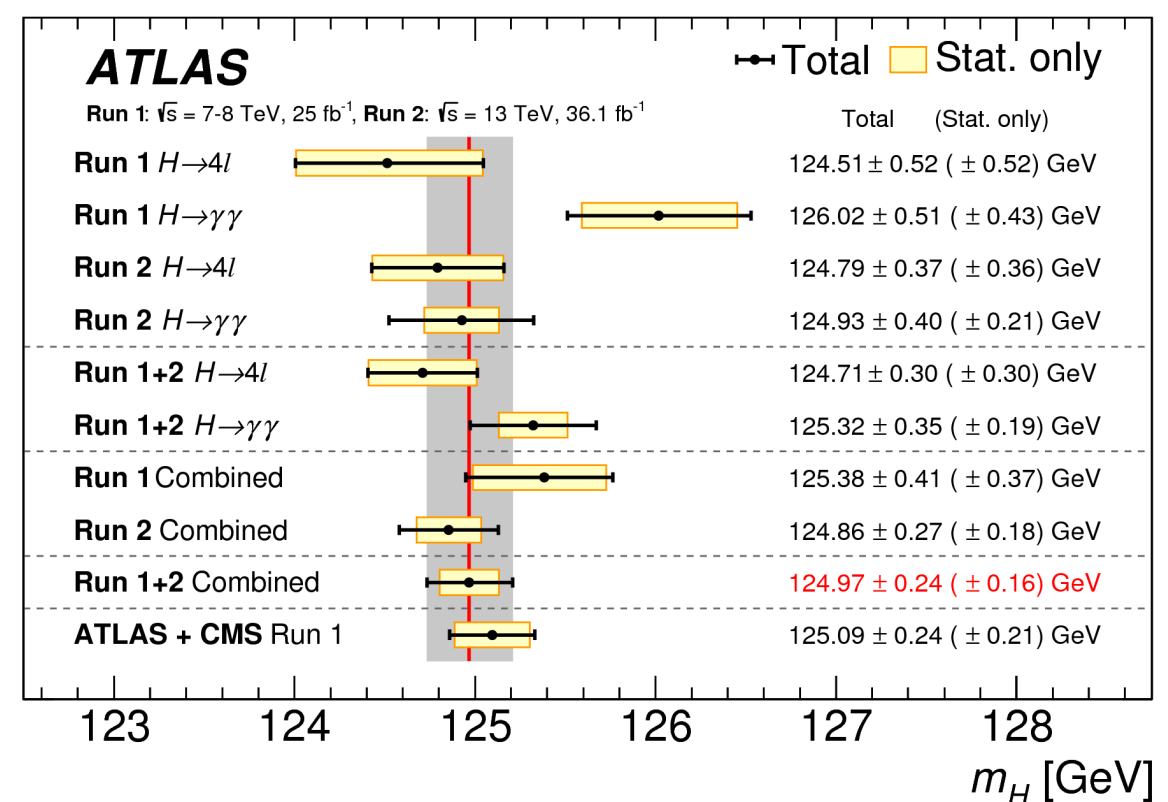
Photon Timing in BSM Search



$H \rightarrow \gamma\gamma$  Peak



Higgs Mass Measurements





# Ongoing Phase I Upgrade

- Run 3 (2021-2024) challenge:

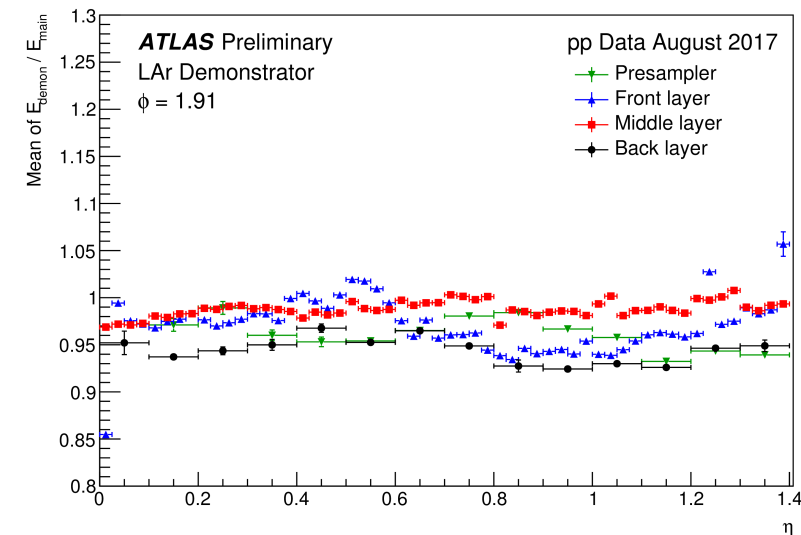
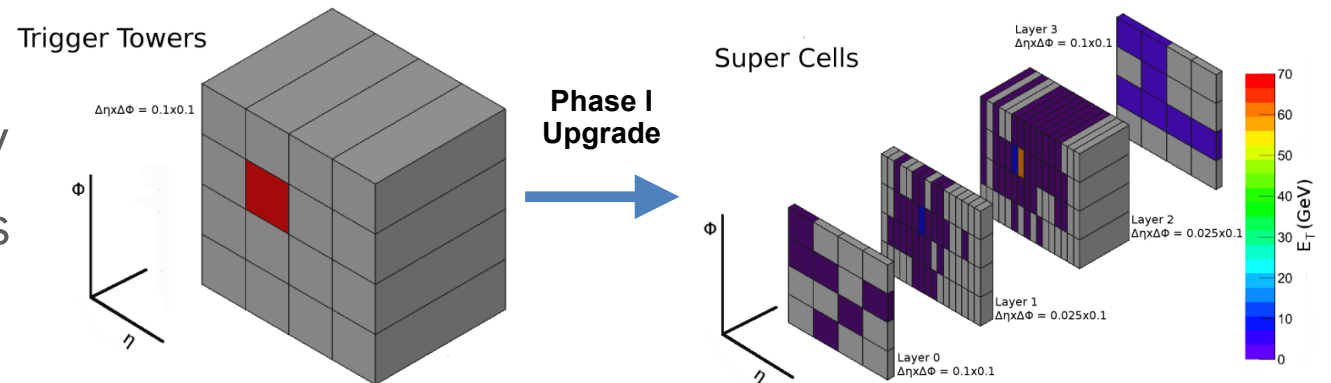
- ▶ Higher pileup and instantaneous luminosity
- ▶ But maintain same Level-1 (L1) trigger rates and thresholds
- ▶ Better discrimination in trigger is needed

- Solution: upgrade of L1 trigger electronics

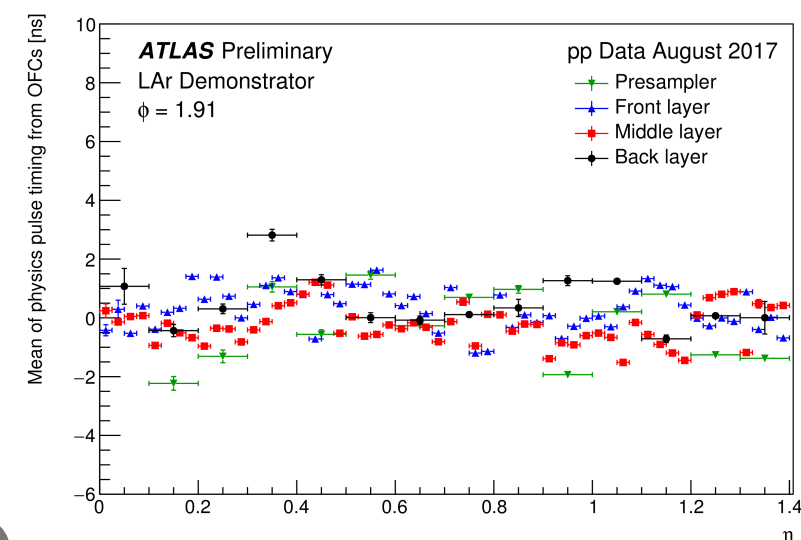
- ▶ 10x greater L1 readout granularity
- ▶ Improved L1 discrimination of  $e, \gamma, \tau$ , jets based on shower shape, isolation, etc.
- ▶ Improved L1 jet  $E_T$  and  $E_T^{\text{miss}}$  resolutions
- ▶ Greatly reduces effects of dominant QCD background and pileup

- Run 2 In-Situ Demonstrators

- ▶ 2 generations of demonstrator systems ran parasitically in the barrel throughout Run 2
- ▶ Validated design, observed good agreement with main readout



Energy Agreement



Time Agreement

# Summary

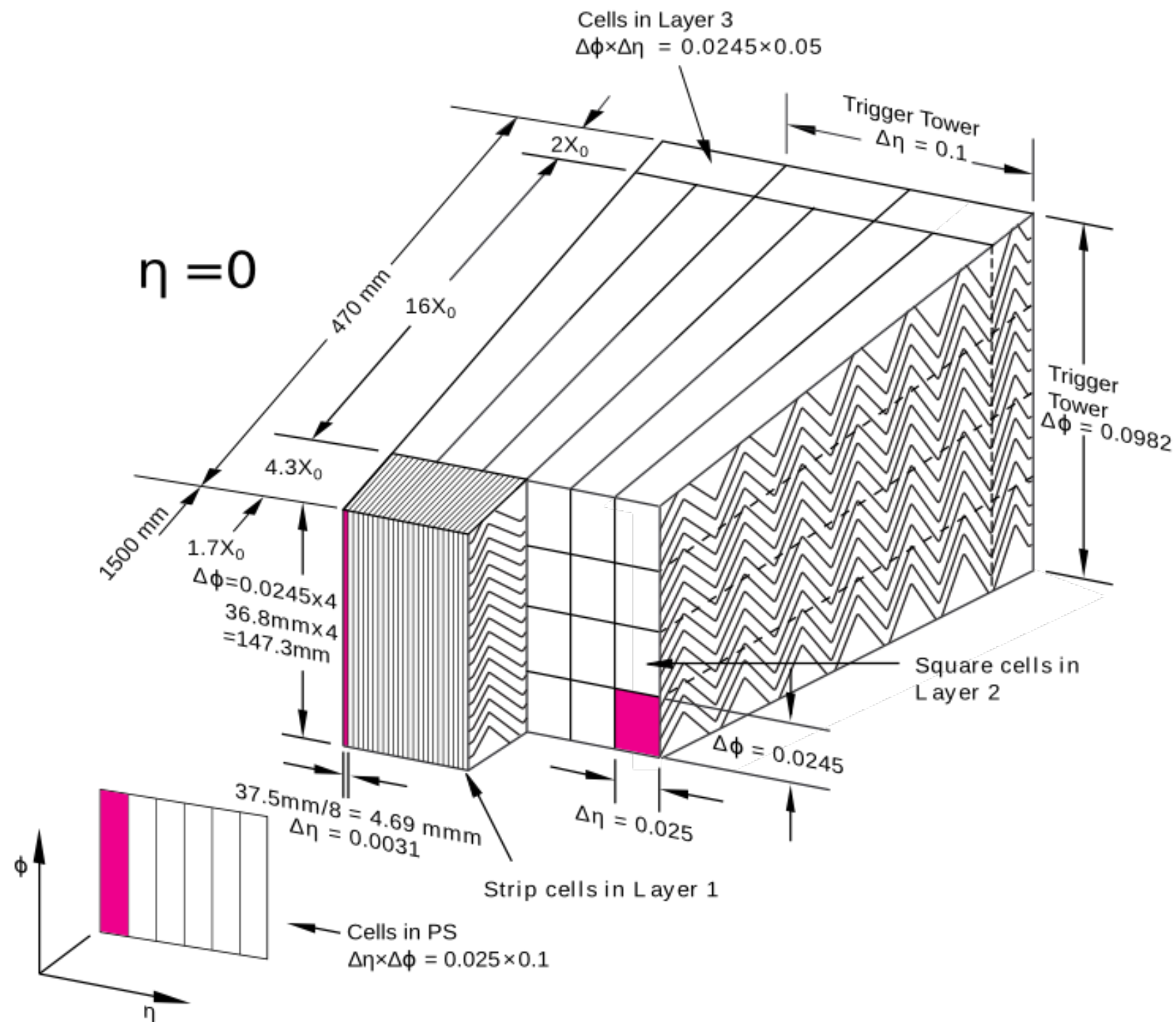


- The ATLAS LAr Calorimeters operated very successfully throughout Run 2 with 99.6% overall data-efficiency
- Various Run 2 studies demonstrate the excellent quality of physics data collected and the commitment to continually improving operations and performance
- LAr has contributed greatly to many important physics measurements and searches during Run 2
- Ongoing upgrades to handle conditions in Run 3 are well underway
  - ▶ Dedicated Phase I and HL-LHC upgrade talks on Friday

# Backup



# Cell Diagram

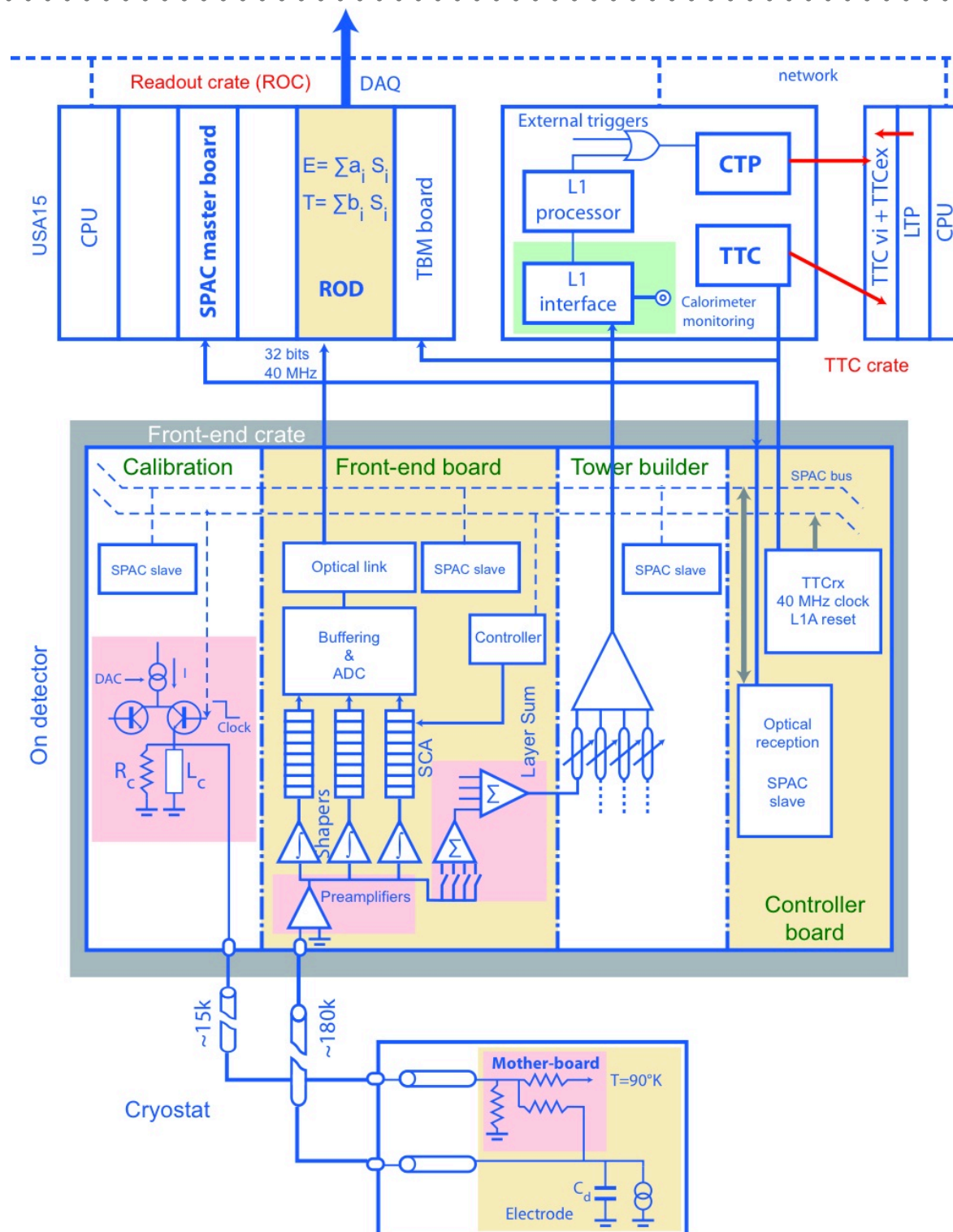


# Energy Resolutions

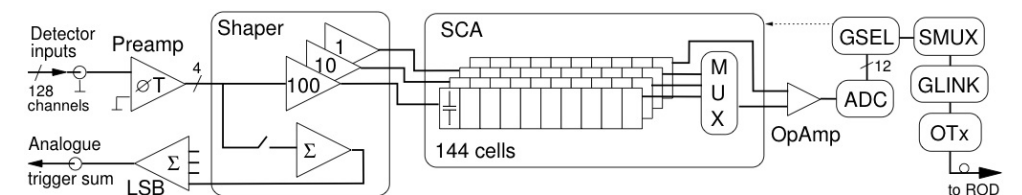
Detector component	Required resolution	$\eta$ coverage	
		Measurement	Trigger
Tracking	$\sigma_{p_T}/p_T = 0.05\% p_T \oplus 1\%$	$\pm 2.5$	
EM calorimetry	$\sigma_E/E = 10\%/\sqrt{E} \oplus 0.7\%$	$\pm 3.2$	$\pm 2.5$
Hadronic calorimetry (jets)			
barrel and end-cap	$\sigma_E/E = 50\%/\sqrt{E} \oplus 3\%$	$\pm 3.2$	$\pm 3.2$
forward	$\sigma_E/E = 100\%/\sqrt{E} \oplus 10\%$	$3.1 <  \eta  < 4.9$	$3.1 <  \eta  < 4.9$
Muon spectrometer	$\sigma_{p_T}/p_T = 10\%$ at $p_T = 1$ TeV	$\pm 2.7$	$\pm 2.4$

**Table 1.** General performance goals of the ATLAS detector. Note that, for high- $p_T$  muons, the muon-spectrometer performance is independent of the inner-detector system. The units for  $E$  and  $p_T$  are in GeV.

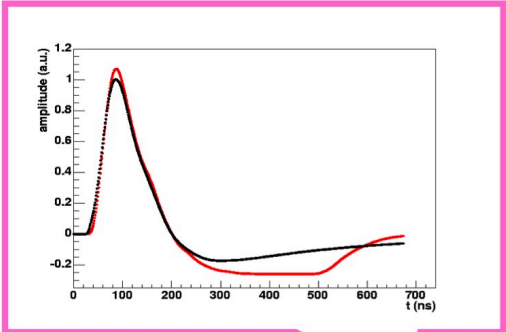
# Readout Electronics Chain



*Front-End Board Schematic*



# Energy Reconstruction



$$E_{\text{cell}} = F_{\mu A \rightarrow \text{MeV}} \cdot F_{DAC \rightarrow \mu A} \cdot \frac{1}{\frac{M_{\text{phys}}}{M_{\text{cali}}}} \sum_{i=1}^{M_{\text{ramps}}} R_i \left[ \sum_{j=1}^{N_{\text{samples}}} a_j (s_j - p) \right]^i$$

Cell energy

Sampling fraction

Calibration board

ADC to DAC (Ramps)

Pulse Samples

Optimal Filtering Coefficients

Pedestals

The above formula describes the LAr electronic calibration chain (from the signal ADC samples to the raw energy in the cell. Note that this version of the formula uses the general  $M_{\text{ramps}}$ -order polynomial fit of the ramps. We use a linear fit as the electronics are very linear, and we only want to apply a linear gain in the DSP in order to be able to undo it offline, and apply a more refined calibration. In this case, the formula is simply:

$$E_{\text{cell}} = F_{\mu A \rightarrow \text{MeV}} \cdot F_{DAC \rightarrow \mu A} \cdot \frac{1}{\frac{M_{\text{phys}}}{M_{\text{cali}}}} \cdot R \left[ \sum_{j=1}^{N_{\text{samples}}} a_j (s_j - p) \right]$$